MNRAS 000, 1–7 (2023) Preprint 19 May 2023 Compiled using MNRAS LATEX style file v3.0

Probing Intracluster Dynamics and Evolution of Globular Clusters through Cataclysmic Variable Populations

Kwangmin Oh,[1] C. Y. Hui,[2]★ Jongsuk Hong[3]† Sangin Kim[1] and Fifth Author[4]
[1]*Department of Space Science and Geology, Chungnam National University, Daejeon 34134, Republic of Korea*
[2]*Department of Astronomy and Space Science, Chungnam National University, Daejeon 34134, Republic of Korea*
[3]*Korea Astronomy and Space Science Institute, Daejeon 34055, Republic of Korea*

Accepted XXX. Received YYY; in original form ZZZ

ABSTRACT

Dynamical interactions in globular clusters (GCs) significantly impact the formation and evolution of binary sources, including cataclysmic variables (CVs). This study investigates the connection between GC dynamical states and X-ray luminosity (L_x) distributions of CV populations. Monte Carlo code called MOCCA identified three GC classes based on evolutionary status. The simulated L_x distributions of CVs display considerable variations among these classes. By analyzing 224 CV candidates in 18 GCs observed by the *Chandra* X-ray Observatory and classifying them according to Ferraro et al. (2012), the L_x distributions also show significant differences. The observational results align with the MOCCA simulations, revealing that CVs in more dynamically evolved clusters (Class/Family III) exhibit brighter X-ray emission. This highlights the impact of GC dynamical status on compact binary properties. Similar to blue stragglers, CV populations can serve as tracers of GC dynamical history. Our findings provide insights into compact binary formation, evolution, and properties in diverse dynamical environments and enhance understanding of intracluster dynamics and binary evolution in GCs.

Key words: Cataclysmic variables – Globular clusters – Compact binaries – Dynamical interaction

1 INTRODUCTION

The complex interplay between the dynamical formation of binary sources including cataclysmic variables (CVs) and the evolution of globular clusters (GCs) remains to be an intriguing topic for many studies over the years (e.g. Ivanova et al. 2006; Hong et al. 2017). CVs are binaries comprised of a white dwarf accretor and a donor star which are typically low-mass main-sequence (MS) stars. Mass transfer occurs when the donor star fills its Roche lobe which leads to the accretion of material on the surface of the white dwarf and gives rise to the X-ray emission. For the CVs hosted by GCs, their formation and evolution can be complicated by frequent stellar encounters. The intracluster dynamics such as tidal capture and exchange interaction (Hut et al. 1992; Pooley & Hut 2006; Belloni et al. 2016a,b, 2017, 2019) can strongly affect the binary properties of CVs in GCs (e.g. mass ratio, orbital separation). This can possibly result in emission properties that differ from those of binaries in an environment without such a dynamical process (e.g. Galactic field). This notion is supported by the recent discovery that some properties of millisecond pulsars in GCs (e.g., X-ray conversion efficiency, rotational period distribution) are significantly different from their counterparts in the Galactic field (Lee et al. 2023), providing evidence for the influence of intracluster dynamics on the evolution of their progenitors (e.g., low-mass X-ray binaries).

While intracluster dynamics can affect the evolution of compact binaries, the presence of such exotic systems in GCs can also influence cluster evolution. Elastic scattering between binary systems and single stars or other binaries can prevent or reverse core collapse by transferring gravitational potential energy to the kinetic energy of stars in the core (Hut et al. 1992). If the initial binding energy of a primordial binary is larger than the average kinetic energy of neighboring stars in a GC, the encounter can lead to orbital shrinkage with the orbital binding energy transferred to neighboring stars (Heggie 1975). This process, commonly referred to as binary-burning, can lead to equipartition among the binding energy of the binaries, recoil kinetic energy of the binaries, and the kinetic energy of the stars. Due to this equipartition of energy, higher-mass stars are scattered to lower velocities and consequently sink to the core. This process, known as mass segregation (Spitzer 1987; Meylan & Heggie 1997), naturally increases the core density, enhancing stellar interactions in the core. All the aforementioned processes illustrate the complexity of co-evolution between GCs and their hosted binaries.

The dynamical status of GCs can be reflected by their morphology. It is widely accepted that GCs can be classified into core-collapsed (CCed) and non-core-collapsed (Non-CCed) according to their core sizes (Harris 1996, 2010 edition). By comparing the results from the core sizes resulting from simulations with the observed values, Fregeau (2008) have suggested that CCed GCs are in the binary-burning phase and most of the Non-CCed GCs are still in the core contraction phase. The author also points out that there can be a significant X-ray source overabundance in CCed GCs. To make such a study more intricate, instead of the aforementioned binomial classification, Ferraro et al. (2012) have suggested GCs can be classified into three distinct groupings according to the radial distributions of blue stragglers (BSs). Using BSs as the probe of GC evolution, these

★ E-mail: huichungyue@gmail.com
† E-mail: jshong@kasi.re.kr

three groupings (referred to as Family I, II, and III hereafter) can reflect the cluster dynamical age.

Given the three-families classification scheme laid down by Ferraro et al. (2012), two questions naturally arise: (1) What is the physical origin of such classification? And (2) Do the properties of X-ray binaries vary across these three families? In this study, we endeavor to address these two questions. To understand whether the evolution of a GC can lead to trifurcation, we utilize Monte Carlo code to explore how cluster properties vary from zero age to present. This approach enables us to examine how the binary population co-evolves with the cluster.

To investigate compact binaries, we will focus on the quiescent X-ray properties of CVs in this work for two reasons. First, in comparison with other classes of compact binaries such as millisecond pulsars, the accretion-powered X-ray emission from CVs can be estimated with a simple model. Furthermore, the luminous and hard X-rays from CVs make them easier to be identified by observations and therefore we can collect an observed sample of CV-like X-ray sources to compare with the simulated results.

In addition to the study of CVs, it is worth noting that white dwarf-white dwarf (WD-WD) binaries, particularly those with short orbital periods, can also play an important role as potential gravitational wave sources. The understanding of the formation and evolution of such systems in dense stellar environments like GCs can significantly contribute to our knowledge of gravitational wave astronomy.

2 PREVIOUS WORKS ON DYNAMICAL FORMATIONS OF CVS IN GCS

The dynamical formation of CVs in GCs has attracted significant attention over the past decades, with numerous studies aiming to better understand the complex interplay between stellar interactions, binary evolution, and the dynamical state of GCs. In the high-density environments of GCs, stellar interactions can significantly influence the formation of X-ray binaries, including CVs (Clark 1975; Hut et al. 1992; Verbunt, F. 2001). This is supported by a strong correlation found between the number of X-ray sources and the encounter rate of GCs, indicating that dynamical interactions play a crucial role in the formation of X-ray binaries (Verbunt & Hut 1987; Pooley et al. 2003; Hui et al. 2010).

Rivera Sandoval et al. (2018) also revealed that core-collapsed GCs tend to have bimodal CV populations in their NUV and optical luminosity. This discovery highlights the significance of comparing CV populations in different types of GCs, such as core-collapsed and non-core-collapsed clusters, to understand the influence of dynamical interactions on CV formation and evolution. By considering these differences and the various dynamical states of GCs, we can gain valuable insights into the processes that govern the formation, destruction, and overall properties of CVs in their different environments.

However, intense encounters between stars can also lead to the evaporation of wide binaries, including CVs, while the GC's tidal field can disrupt CVs on low-angular momentum orbits (Heggie 1975; Hills 1975; Mardling & Aarseth 2001). The formation and destruction of CVs in GCs are complex processes involving various factors such as mass transfer, common envelope evolution, and binary parameters, including mass ratio, separation, and eccentricity (Paczynski 1976; Iben & Livio 1993).

To further investigate the role of dynamical interactions in the formation and destruction of CVs in GCs, researchers have employed Monte-Carlo code. These simulations have demonstrated that stellar interactions in dense core regions of GCs could play a critical role in shaping the CV population (Ivanova et al. 2005; Hong et al. 2017; Belloni et al. 2016a, 2019). However, accurately predicting the CV population based solely on the categorization of core-collapsed and non-core-collapsed GCs has proven to be challenging due to the complex internal dynamics of GCs (Pryor & Meylan 1993; Fregeau et al. 2009; Kremer et al. 2019).

These previous works on the dynamical formation of CVs in GCs have established the importance of considering the intricate interplay between the dynamical state of a GC and the properties of its hosted CVs. The findings of these studies lay the foundation for the investigation presented in this paper, in which we utilize Monte Carlo code and observational data to further explore the connection between the dynamical state of GCs and the X-ray properties of their CV populations.

3 GLOBULAR CLUSTER SIMULATION

3.1 MOCCA

In order to explore the relationship between the dynamical state of GCs and the properties of their CV populations, we conducted Monte Carlo code using the MOCCA code. MOCCA is an effective tool for simulating star cluster evolution, accounting for both stellar dynamics and stellar evolution processes (Giersz et al. 2013). We created 81 GC models with varying initial conditions, representing a broad range of plausible GC configurations. The initial conditions for our 81 GC models included variations in binary fraction, galactocentric distance, the initial number of particles, and the cluster's half-mass radius. These parameters were selected based on their potential influence on the dynamical state of GCs and the properties of CV populations.

We set up the MOCCA simulations as follows:

- *Initial number of particles:* We simulated GCs with initial particle numbers of 200K, 500K, and 1M to represent the range of GC sizes in the Milky Way.
- *Galactocentric distance:* We varied the galactocentric distances of the simulated GCs (4, 8, and 16 kpc) to examine the effects of tidal forces and the Galactic potential on the dynamical evolution of the clusters and the properties of their CV populations.
- *Half-mass radius of the cluster:* We considered initial half-mass radii of 1, 2, and 4 pc to account for the potential influence of the initial density profile on dynamical interactions and the properties of the CV populations in GCs.
- *Binary fraction:* We considered initial binary fractions of 10%, 20%, and 50% to account for the potential impact of the proportion of binary stars on dynamical interactions and CV formation in GCs.

We collected CVs with binaries consisting of WD and MS stars, selecting those CVs that exhibited Roche lobe overflow (RLOF) as they are particularly relevant for understanding the dynamical evolution of GCs. These CVs were labeled for further analysis.

To study the X-ray luminosity of each identified CV, we calculated their luminosities based on the properties of their donor and WD components. Following Belloni et al. (2016a), we calculated the X-ray luminosity for slowly rotating WDs in the [0.5 – 10 keV] band:

$$L_{\rm X} = \varepsilon \frac{G M_{\rm WD} \dot{M}_{\rm dQ}}{2 R_{\rm WD}} \quad (1)$$

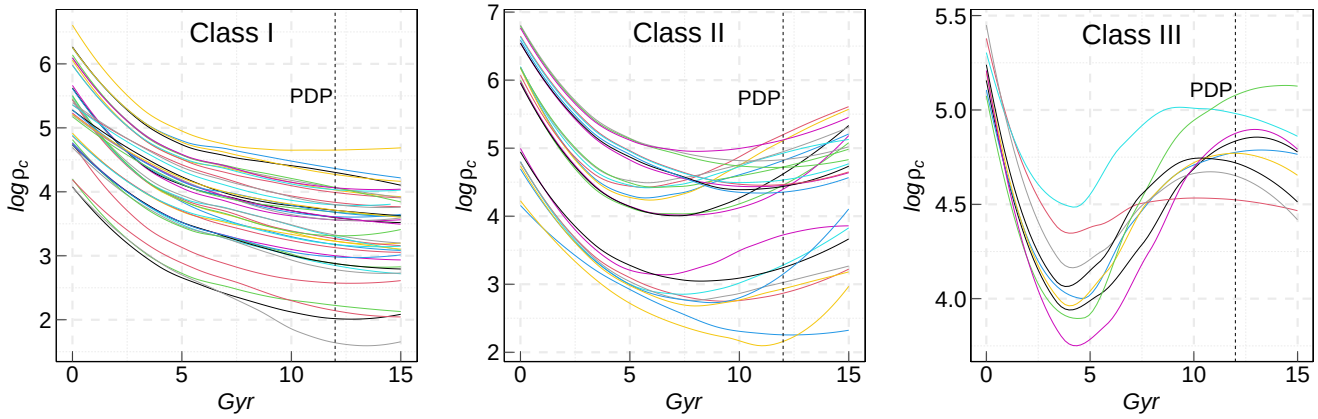

Figure 1. Division of simulated models based on its core density, illustrating the evolution of CV populations in GCs. The three classes display the overall trends of core density over time, reflecting the different dynamical states of the clusters. The dotted line represents the present-day population (PDP) at 12 Gyr, serving as a reference point for comparing the behavior of CV populations in relation to the dynamical history of their host clusters.

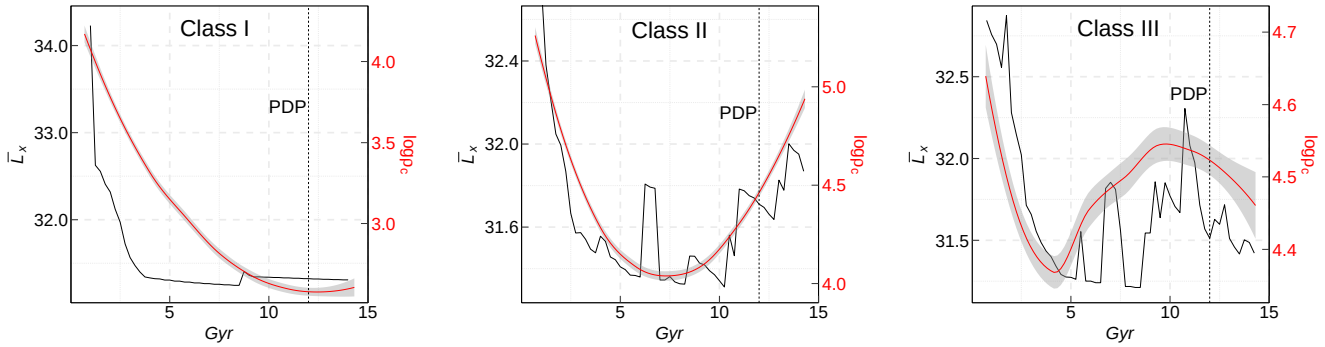

Figure 2. An evolutionary profile of $\bar{L}_x$ and core density over time for simulated GC models, illustrating the impact of dynamical state on CV populations. In each panel, a representative model from each class is selected to visualize CV formation, reflecting the behavior of CVs in clusters with varying dynamical histories. Both Class II and Class III exhibit bright CV formation during the collapsing stage, emphasizing the influence of dynamical interactions on CV properties. The dotted line indicates the present-day population (PDP) at 12 Gyr, serving as a reference point for assessing the evolution of CV populations in relation to the dynamical state of their host clusters.

The factor ε, which is also designated as 0.5, follows the precedent set by Belloni et al. (2016a). In order to model CVs in MOCCA, Belloni et al. (2016a) utilized equation from Lasota (2001). Therefore, the mass transfer rate $\dot{M}_{\rm A}$ establishes the limit between cold/neutral/stable and unstable discs:

$$\dot{M}_{\rm A} = 6.344 \times 10^{-11}\ \alpha_{\rm c}^{-0.004} \left(\frac{M_{\rm WD}}{\rm M_\odot}\right)^{-0.88} \times \left(\frac{r}{10^{10}\ \rm cm}\right)^{2.65} \rm M_\odot\ yr^{-1} \quad (2)$$

3.2 Simulated GC Analysis

In our analysis of the 81 simulated GC models generated using the MOCCA code, we identified three distinct groups based on the core density evolution over time. Core density evolution is essential for understanding the dynamics of GCs, since it provides insights into the interactions and long-term behavior of the constituent stars. We specifically examined the present-day population (PDP) at 12 Gyr, focusing on the core density curve to facilitate easy comparison. (see Fig. 1).

The three groups were classified as follows:

- *Class I:* Models with decreasing core density over time
- *Class II:* Models with increasing core density over time
- *Class III:* Models with saturated core density before PDP

Furthermore, we discovered that a large fraction of bright CVs emerged during the core contraction phase, represented by Group II, and gradually saturated in phases such as Group III. In Fig. 2, three panels illustrate the formation of bright CVs with a representative model in each class.

We gathered and examined the CV populations at PDP for each group, comparing their empirical cumulative distribution functions (eCDFs). As shown in Fig. 3, our analysis of the X-ray luminosity eCDFs reveals notable disparities between the populations. To evaluate the possible divergence and its importance, we utilized a two-sample Anderson-Darling (A-D) test. Our methodology involves determining if the A-D test's p-values are under 0.05 to confirm a significant distinction between two eCDFs. The A-D test results are presented in Table 1. Among the three groups, Group III, considered

Class I vs Class II[1]	Class I vs Class III[1]	Class II vs Class III[1]
5.8×10^{-9}	1.3×10^{-5}	0.44
Family I vs Family II[2]	**Family I vs Family III[2]**	**Family II vs Family III[2]**
0.043	2.4×10^{-6}	2.9×10^{-4}

[1] Three different populations of simulated GCs divided by its central density
[2] Dynamical-age family by Ferraro et al. (2012)

Table 1. Null hypothesis probabilities of the A-D test for comparing X-ray luminosity distributions among three different populations within both simulations and observations. Three distinct classes are derived from the simulations, and three separate families are obtained from the observations.

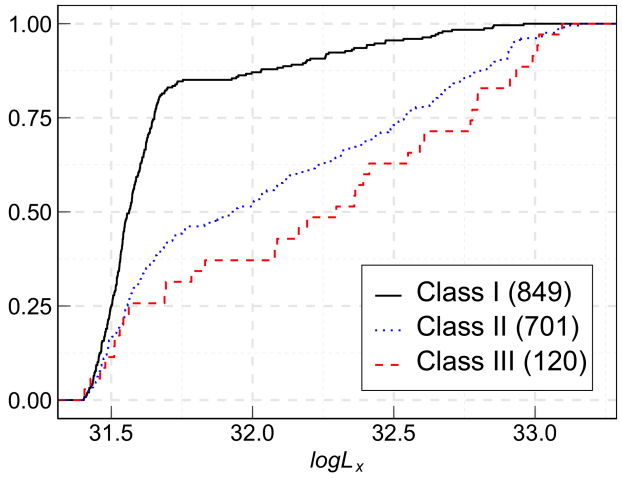

Figure 3. eCDF of X-ray luminosity for the three distinct CV populations, classified according to their core density profiles, highlighting the substantial differences between the groups. Among the three families, Group III, considered the most dynamically evolved population, displays the most luminous CV population, emphasizing the influence of the dynamical state on the properties of CVs. The bracketed numbers in the legends indicate the corresponding sample sizes of collected CVs.

to be the most dynamically old population, displayed the most luminous CV population. Although we observed clear differences in p-values for class I vs. class II and class I vs. class III, the p-values between class II and class III did not meet our objective (> 0.05).

4 X-RAY OBSERVATION

Having established through our MOCCA simulations that GCs can be categorized into three stages based on core density, we sought to validate this finding using observational data. In this section, we will discuss the data collection process, data processing techniques, and the method used to analyze the X-ray luminosity of the GCs. Furthermore, we will explore how the Gaussian Mixture Model (GMM) clustering algorithm allowed us to expand our sample size and better understand the distribution of CV populations within the GCs.

4.1 X-ray data analysis

We obtained X-ray observations of 18 GCs from the Chandra X-ray Observatory, as detailed in Ferraro et al. (2012), and included observations of two additional GCs, NGC 6397 and NGC 6656, for a total dataset of 20 GCs (see Table 2).

ID	Name	ObsID	Family
GCs in Ferraro et al. (2012)			
ω-Cen	NGC 5139[a]	1519, 13726, 13727	I
-	NGC 2419	10490	I
47 Tuc	NGC 104[b]	78, 953, 954, 955, 966, 2735, 2736, 2737, 2738, 3384, 3385, 3386, 3387, 15747, 15748, 16527, 16528, 16529, 17420, 26229, 26286	II
-	NGC 6752[c]	948, 6612, 19013, 19014, 20121, 20122, 20123	II
M 3	NGC 5272[d]	4542, 4543, 4544	II
M 4	NGC 6121[e]	946, 7446, 7447	II
M 13	NGC 6205	5436, 7290	II
M 92	NGC 6341	3778, 5241	II
-	NGC 6388[f]	5505, 12453	II
-	NGC 288[g]	3777	II
M 53	NGC 5024	6560	II
M 5	NGC 5904[d]	2676	II
M 10	NGC 6254	16714	II
M 55	NGC 6809[h]	4531	II
M 2	NGC 7809	8960	II
M 30	NGC 7099[i]	2679, 18997, 20725, 20726, 20731, 20732, 20792, 20795, 20796	III
M 79	NGC 1904	9027	III
M 80	NGC 6093	1007	III
Additional GCs			
-	NGC 6397[j]	79, 2668, 2669, 7460, 7461	-
M 22	NGC 6656[k]	5437, 14609	-

CV references:
[a] Henleywillis et al. (2018), [b] Heinke et al. (2005),Rivera Sandoval et al. (2018), [c] Forestell et al. (2014), [d] Tweddale (2021), [e] Bassa et al. (2004), [f] Maxwell et al. (2012), [g] Kong et al. (2006), [h] Bassa, C. G. et al. (2008), [i] Lugger et al. (2007), [j] Cohn et al. (2010), [k] Webb, N. A. & Servillat, M. (2013).

Table 2. ObsIDs of Chandra X-ray Observatory for total 20 GCs in this study. The data set forms the foundation for the analysis of X-ray luminosities and the investigation of CV populations in relation to their host GCs.

For data processing, we analyzed the aforementioned dataset directly by using CIAO (v.4.15.1). With the recently updated calibration database (CALDB v.4.10.4), each observation data were reprocessed by using the `chandra_repro`. Since we took the half-mass radius of the GC into account, we spatially filtered with the region of the half-mass radius field of view by using `dmcopy` before the source detection. For data with multiple ObsIDs, we merged a number of observations for detecting photon counts with high significance by using `merge_obs` with `binsize=0.5` for the subpixel resolution analysis. To construct the point source list for each GC, we ran the wavelet detection algorithm of `wavdetect` on merged data with the

`scales="1, 1.414, 2, 2.828"` as long as the significance of detected sources is larger than the threshold of `sigthresh=1e-5`. For those identified as X-ray sources, by assuming that all sources in one GC locate at the same distance as the corresponding GC's distance from Earth, the luminosity of each source was calculated by using `srcflux` over energy bands of 0.3-1.5 keV (soft; s), 1.5-7.0 keV (hard; h), and 0.3-7.0 keV with the effective energy of 0.9, 3.6, and 1.9 keV, respectively. Consequently, the aforementioned procedure results in 763 X-ray sources.

Among the X-ray sources identified through data processing, 66 sources were confirmed as CVs via optical counterpart analysis (refer to the footnotes in Table 2 for details). This includes 54 sources from Ferraro et al. (2012) and 12 additional sources. However, given that the sample size was insufficient for our study, we applied a GMM clustering algorithm to the X-ray colour-luminosity diagram in order to expand the number of CV candidates. The GMM algorithm is a probabilistic model that attempts to fit a mixture of Gaussian distributions to the input data, estimating the mean and covariance of each Gaussian component. By doing so, it can effectively identify underlying patterns and group data points into distinct clusters. The GMM clustering analysis led to the identification of four distinct groups, with the majority of confirmed CVs (~71.4%) residing in one specific cluster. By assigning CV labels to potential CV candidates located in the same cluster as the confirmed CVs, it enable us to increase our number of CV from 66 to 224.

Fig. 4 illustrates the division of the four clusters using the GMM algorithms. The subfigure on the top shows the GMM clustering results with different colours representing the distinct groups. The subfigure in the middle demonstrates the distribution of the 66 confirmed CVs on the X-ray colour-luminosity diagram before applying the GMM algorithm. Finally, the subfigure at the bottom displays the expanded CV population after employing the GMM, including both the confirmed CVs and the newly identified CV candidates. This approach enhances the statistical power of our analysis by increasing the sample size and allows for a more comprehensive investigation of CV populations in the selected GCs.

Building upon Ferraro et al. (2012), we conducted an analysis using X-ray luminosity eCDFs of CVs in the GCs listed by them. Our investigation encompassed a total of 224 CV candidates from 18 GCs, resulting in the identification of 44, 161, and 19 CVs for families I, II, and III, respectively. To better understand the nature of these CV populations, we performed a comparative analysis of their X-ray luminosities. We hypothesized that variations in X-ray brightness could provide insights into the underlying properties and evolutionary stages of these CV populations.

Fig. 5 displays the X-ray luminosity eCDFs, revealing differences among the three CV populations, which suggests significant variations in X-ray brightness. These variations may be attributed to differences in accretion rates, magnetic field strengths, or mass transfer processes within the CV systems, possibly linked to their respective dynamical-age families. As indicated in Table 1, the A-D test confirmed significant differences ($p < 0.05$) among all three dynamical GC families. This information not only enhances our understanding of CV population distribution within GCs but also sheds light on their evolutionary stages.

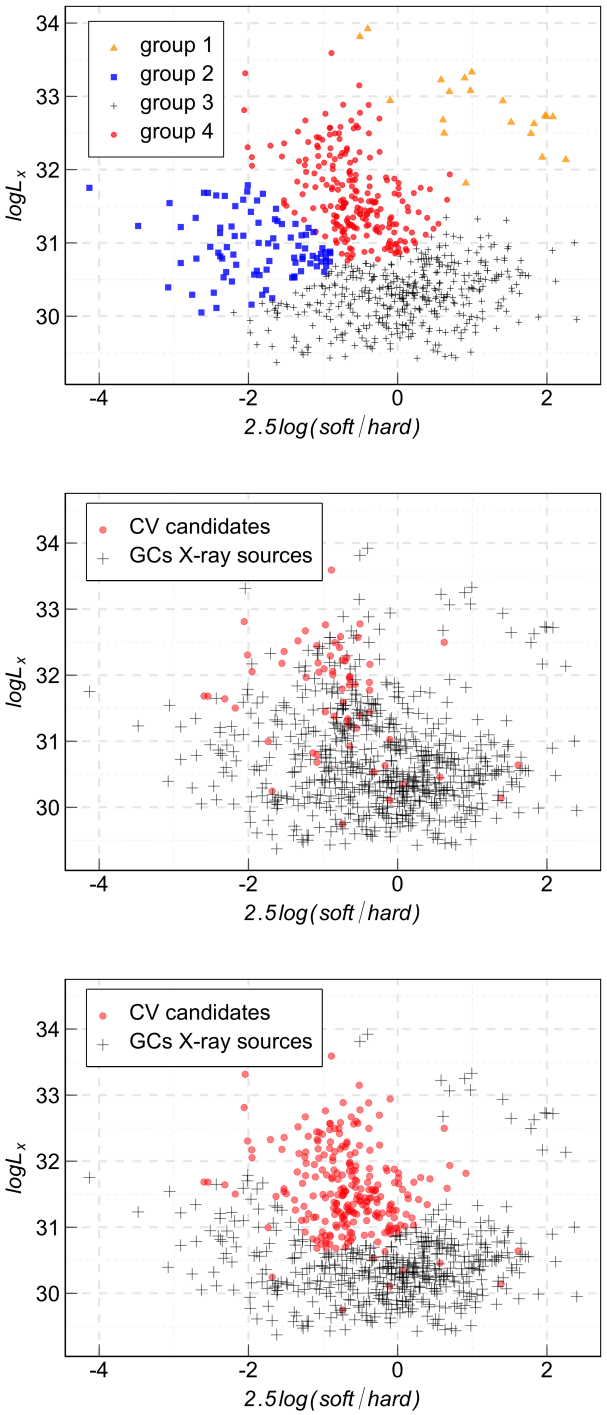

Figure 4. GMM clustering applied to the X-ray colour-luminosity diagram. Top panel: Four distinct groups identified through GMM clustering, represented by different colours. Middle panel: The 66 confirmed CVs plotted on the X-ray colour-luminosity diagram prior to GMM implementation. Bottom panel: The enlarged CV population after using GMM, consisting of both confirmed CVs and new CV candidates. This method expands the sample size, facilitating a thorough examination of CV populations in selected 20 GCs.

5 SUMMARY & DISCUSSION

In this study, we have investigated the relationship between the dynamical states of GCs and the properties of their CV populations,

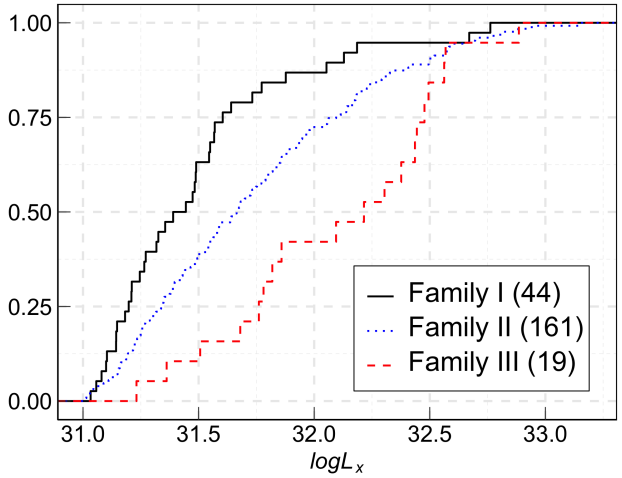

Figure 5. eCDF of X-ray luminosity for the three different populations of CV candidates in GCs. The dynamically older population (Family III) exhibits the brightest CV candidates among the three families, highlighting the impact of the dynamical state on the properties of CVs. The bracketed numbers in the legends show the corresponding sample sizes of CV candidates.

using the MOCCA code and observational data analysis. Our main findings can be summarized as follows:

1. We identified three distinct dynamical-age families in the observational data, as well as in our simulated GC models, based on the core density evolution over time and the distribution of CV populations within the GCs.

2. The X-ray luminosity of CVs was found to be brighter in more dynamically evolved GCs (Family III), consistent between Monte Carlo code results and our observational data, suggesting a crucial role of the dynamical state of GCs in determining the properties of CVs.

3. Our findings support the idea that CVs, like BSs, can effectively probe GCs' dynamical states, enhancing our understanding of CV and BS formation, evolution, and properties across various dynamical environments.

The strong link between the properties of CVs and the dynamical state of GCs, as well as the similarity in the processes that govern the formation and evolution of both CVs and BSs, highlights the significant potential of CVs as valuable tracers of the dynamical history of GCs. By deepening our understanding of these relationships, our findings hold the potential to significantly impact the field of GC research and contribute to a more comprehensive picture of the formation, evolution, and properties of CVs and BSs in diverse dynamical environments.

While our study offers important insights into the relationship between GC dynamical state and CV populations, there are some limitations that warrant acknowledgment. Although the sample size of GCs and CVs is substantial, expanding it would provide further validation of our findings. Additionally, the MOCCA code employed in our simulations might not capture certain complex processes that influence CV properties within GCs. Moreover, assumptions and simplifications made in our study, such as those concerning magnetic fields in mCVs, could impact the accuracy of our conclusions. Addressing these limitations in future research will help refine our understanding of the interplay between GC dynamics and CV populations.

Building upon our findings, future research should focus on increasing the sample of GCs and CVs to offer a more comprehensive perspective on the relationship between cluster dynamical state and CV population properties. Furthermore, detailed theoretical modeling of physical processes governing CV formation and evolution in diverse dynamical environments, including the role of magnetic fields in mCVs, could shed light on the underlying mechanisms responsible for observed trends in X-ray luminosity.

6 CONCLUSION

In this study, we have explored the relationship between the dynamical state of GCs and the properties of their CV populations. By analyzing 224 CV candidates in 20 GCs classified into three different dynamical ages and performing simulations with 81 simulated GC models, we have demonstrated a clear connection between the dynamical state of GCs and the X-ray luminosity of their CVs.

Our investigation enhances our understanding of the complex interplay between the dynamics of GCs and the characteristics of their constituent stars, including CVs and BSs. Future research directions include expanding the sample of GCs and CVs, providing a more comprehensive view of the relationship between the dynamical state of clusters and the properties of their CV populations. Moreover, detailed theoretical modeling of the physical processes governing CV formation and evolution in various dynamical environments could help further elucidate the underlying mechanisms responsible for the observed trends in X-ray luminosity.

ACKNOWLEDGEMENTS

K.OH is supported by the National Research Foundation of Korea grant 2022R1A6A3A13071461. C.Y.H. is supported by the research fund of Chungnam National University and by the National Research Foundation of Korea grant 2022R1F1A1073952.

DATA AVAILABILITY

The data underlying this article were accessed from Chandra Data Archive (https://cda.harvard.edu/chaser/).

REFERENCES

Bassa, C. G. Pooley, D. Verbunt, F. Homer, L. Anderson, S. F. Lewin, W. H. G. 2008, A&A, 488, 921
Bassa C., et al., 2004, The Astrophysical Journal, 609, 755
Belloni D., Giersz M., Askar A., Leigh N., Hypki A., 2016a, Monthly Notices of the Royal Astronomical Society, 462, 2950
Belloni D., Giersz M., Rocha-Pinto H. J., Leigh N. W. C., Askar A., 2016b, Monthly Notices of the Royal Astronomical Society, 464, 4077
Belloni D., Zorotovic M., Schreiber M. R., Leigh N. W. C., Giersz M., Askar A., 2017, Monthly Notices of the Royal Astronomical Society, 468, 2429
Belloni D., Giersz M., Rivera Sandoval L. E., Askar A., Ciecieląg P., 2019, Monthly Notices of the Royal Astronomical Society, 483, 315
Clark G. W., 1975, ApJ, 199, L143
Cohn H. N., et al., 2010, The Astrophysical Journal, 722, 20
Ferraro F. R., et al., 2012, Nature, 492, 393–395
Forestell L. M., Heinke C. O., Cohn H. N., Lugger P. M., Sivakoff G. R., Bogdanov S., Cool A. M., Anderson J., 2014, Monthly Notices of the Royal Astronomical Society, 441, 757
Fregeau J. M., 2008, ApJ, 673, L25
Fregeau J. M., Ivanova N., Rasio F. A., 2009, The Astrophysical Journal, 707, 1533
Giersz M., Heggie D. C., Hurley J. R., Hypki A., 2013, MNRAS, 431, 2184

Harris W. E., 1996, AJ, 112, 1487
Heggie D. C., 1975, MNRAS, 173, 729
Heinke C. O., Grindlay J. E., Edmonds P. D., Cohn H. N., Lugger P. M., Camilo F., Bogdanov S., Freire P. C., 2005, The Astrophysical Journal, 625, 796
Henleywillis S., Cool A. M., Haggard D., Heinke C., Callanan P., Zhao Y., 2018, Monthly Notices of the Royal Astronomical Society, 479, 2834
Hills J. G., 1975, AJ, 80, 809
Hong J., Vesperini E., Belloni D., Giersz M., 2017, MNRAS, 464, 2511
Hui C. Y., Cheng K. S., Taam R. E., 2010, The Astrophysical Journal, 714, 1149
Hut P., et al., 1992, PASP, 104, 981
Iben Icko J., Livio M., 1993, PASP, 105, 1373
Ivanova N., Belczynski K., Fregeau J. M., Rasio F. A., 2005, Monthly Notices of the Royal Astronomical Society, 358, 572
Ivanova N., Heinke C. O., Rasio F. A., Taam R. E., Belczynski K., Fregeau J., 2006, Monthly Notices of the Royal Astronomical Society, 372, 1043
Kong A. K. H., Bassa C., Pooley D., Lewin W. H. G., Homer L., Verbunt F., Anderson S. F., Margon B., 2006, The Astrophysical Journal, 647, 1065
Kremer K., Chatterjee S., Ye C. S., Rodriguez C. L., Rasio F. A., 2019, The Astrophysical Journal, 871, 38
Lasota J.-P., 2001, New Astron. Rev., 45, 449
Lee J., Hui C. Y., Takata J., Kong A. K. H., Tam P.-H. T., Li K.-L., Cheng K. S., 2023, The Astrophysical Journal, 944, 225
Lugger P. M., Cohn H. N., Heinke C. O., Grindlay J. E., Edmonds P. D., 2007, The Astrophysical Journal, 657, 286
Mardling R. A., Aarseth S. J., 2001, MNRAS, 321, 398
Maxwell J. E., Lugger P. M., Cohn H. N., Heinke C. O., Grindlay J. E., Budac S. A., Drukier G. A., Bailyn C. D., 2012, The Astrophysical Journal, 756, 147
Meylan G., Heggie D., 1997, Astronomy and Astrophysics Review, 8, 1
Paczynski B., 1976, Symposium - International Astronomical Union, 73, 75–80
Pooley D., Hut P., 2006, ApJ, 646, L143
Pooley D., et al., 2003, The Astrophysical Journal, 591, L131
Pryor C., Meylan G., 1993, in Djorgovski S. G., Meylan G., eds, Astronomical Society of the Pacific Conference Series Vol. 50, Structure and Dynamics of Globular Clusters. p. 357
Rivera Sandoval L. E., et al., 2018, Mon. Not. Roy. Astron. Soc., 475, 4841
Spitzer L., 1987, Dynamical evolution of globular clusters
Tweddale J. D., 2021, Master's thesis, San Francisco State University, doi:10.46569/20.500.12680/gf06g798f
Verbunt F., Hut P., 1987, IAU Symposium, 125, 187
Verbunt, F. 2001, A&A, 368, 137
Webb, N. A. Servillat, M. 2013, A&A, 551, A60

This paper has been typeset from a TEX/LATEX file prepared by the author.